

# Optical measurement method for dynamic mechanical testing based on image grey level distribution difference model

Zhiqiang Yin<sup>1, 2\*</sup>, Lei Wang<sup>1, 2</sup>, Haifeng Ma<sup>3</sup>

<sup>1</sup>The Provincial Key Laboratory of mining effects and disasters preventing under deep mining in Anhui, Anhui University of Science and Technology, Huainan, Anhui, China, 232001

<sup>2</sup>School of Mineral and Safety, Anhui University of Science and Technology, Huainan, Anhui, China, 232001

<sup>3</sup>Faculty of Resources and Safety Engineering, China University of Mining and Technology, Beijing, China, 100083

Received 26 October 2013, www.tsi.lv

## Abstract

This study developed an optical measuring system with a gray level distribution difference (GLDD) model, and applied the system to examine the displacement field of a Brazilian disk (BD) split under dynamic loading. The system consists of high-speed (HS) photography, a split-Hopkinson pressure bar (SHPB), a synchronization control system and operation of differential images. First, we captured differential images with a high speed camera (10 frames at a time resolution of 10 $\mu$ s). Next, we established the corresponding relationship between the dynamic fracturing evolution of the disc rock samples and the stress loading process with a synchronization controlling system. Changes in the surface displacement field were calculated with the differential image base method according to the joint probability distribution function of two images. This method takes the image correlation into account and can effectively eliminate the influence of background noise, identify surface displacement and capture cracks and expansion in dynamic Brazilian disk splitting experiments straightforwardly and accurately. Findings can be used for novel measurement of surface displacement fields in Brazilian disk splitting tests under dynamic loads.

*Keywords:* grey level distribution difference model, SHPB, dynamic load, high speed photography, differential image

## 1 Introduction

In recent years, computer digital imagery has been widely used to measure full-field deformation in material and structure mechanics [1]. Recently, new static loading test procedures have been developed to calculate surface displacement and deformation based on digital images of good quality with standard cameras [2]. However, in dynamic loading tests (impact, Hopkinson bar tests), relatively small, higher resolution images are required for the displacement measurement. So far, the development of methods that handle dynamic events is still in its infancy [3].

Traditional contact measurement techniques using sensors such as mechanical extensometers and strain gauges have limitations in frequency response and measuring range. Therefore, they cannot provide sufficient information to explore the rapid variation of dynamic mechanical behaviours. Non-contact, full-field monitoring techniques such as caustics, Moiré, photo elasticity, digital image correlation and coherent gradient sensors have substantial advantages for measuring deformation and stress fields in dynamic loading tests [4]. However, most of these techniques require many optical components. These are often quite expensive, and are only applicable for transparent materials such as organic polymers and inorganic glass. They are not suitable for

deformation measurements in rock dynamic experiments.

Many studies have explored deformation and crack characteristics of rock materials under dynamic loading [5, 6]. High-speed cameras and digital image methods have been developed in recent years. For example, Siviour used a high speed camera for a high strain rate experiment to monitor specimen deformation and analyse field methods for three point bending. Louis Ngai Yuen Wonga used digital image subtraction techniques to inspect cracking processes in Carrara marble specimens containing a single, pre-existing open flaw under dynamic loading.

Digital image subtraction is a common tool to analyse image changes. With this standard tool, most researchers are already familiar with resulting difference images. Taking a simple subtraction between two images is directly equivalent to forming a null hypothesis test statistic, assuming that the expected change is due to uniform noise. Therefore, this can be described by a single distribution across the entire image [7]. However, the background noise in dynamic experiments of digital images is uneven, and is affected by light sources and camera equipment. Therefore, an effective processing technique is essential to remove background noise from dynamic load images.

In this work, Brazilian disc specimens were loaded with a SHPB system, and a high-speed camera was used

\* Corresponding author e-mail: zhqyin@aust.edu.cn

to monitor the full-field dynamic fracture process in the specimens. Surface deformation and failure mode of specimen were analysed, based on the grey level distribution difference (GLDD) model.

**2 GLDD model**

The GLDD model is used to calculate difference images using probability distributions in the normalized scatter gram. This defines a probability that reflects how likely it is that grey level values from corresponding pixels in an image pair are drawn from the same distribution as the rest of the data. Corresponding pairs of pixels from original images are taken, and their grey levels are used to find their coordinates in the normalized scatter gram [7]. Integration is then performed along the vertical cut passing through that point *c*, summing all of the values *F(x, y)* that are smaller than the value of *F(x, c)* at that point.

$$D(x, y) = \sum_c \delta(F(x, c) > F(x, y)) F(x, c) . \quad (1)$$

The images of *g<sub>1</sub>(x, y)* and *g<sub>2</sub>(x, y)* are the grey values of the subset in the non-deformed and deformed images, respectively. The variable *m* and *n* are the probability distribution density of the grey values of images, respectively. *S(m, n)* is probability distribution of the pixel gray distribution with *g<sub>1</sub>* and *g<sub>2</sub>*. The image difference *S* can reflect the probability of grey values different between two images in the same region. Therefore, when the image of *g<sub>1</sub>(x, y)* and *g<sub>2</sub>(x, y)* are completely identical, *S*=0. When the background noise of images shows no change, *S* is the direct finite difference, such as:

$$S = abs[g_1(x, y) - g_2(x, y)] . \quad (2)$$

When the background noise of images changes, *S* are equal to stack values of the weighted average background noise and grey. This eliminates the effect of background noise.

**3 Test systems**

The experimental set up for the SHPB impact test in this study is shown in Figure 1. The SHPB system consisted of a gas gun, a conical bullet, and a stress transmission component [8]. A conical bullet was used in the improved test system to eliminate oscillation and obtain a stable half-sine wave loading [9]. The stress transmission component was made up of three elastic bars, including an incident bar (2m in length), a transmission bar (1.5m), and a momentum bar (0.7m). The rock specimen was sandwiched between the incident bar and the transmission bar. The conical bullet and elastic bars made from 50 mm diameter high strength steel (40Cr), and have yield strength of 800MPa. Two sets of strain gauges are glued on the surface of the middle of the incident bar (SG<sub>in</sub>) and the transmission bar (SG<sub>Tr</sub>) respectively. Each set

consisted of two gauges in a symmetrical arrangement. These strain gauges are used to measure the strain histories induced by the stress waves propagating along the elastic bars. The strain history during the test was recorded with a digital oscilloscope (DL 750) though a differential amplifier (super dynamic meter CS-1D) and a Wheatstone bridge connected to strain gauges.

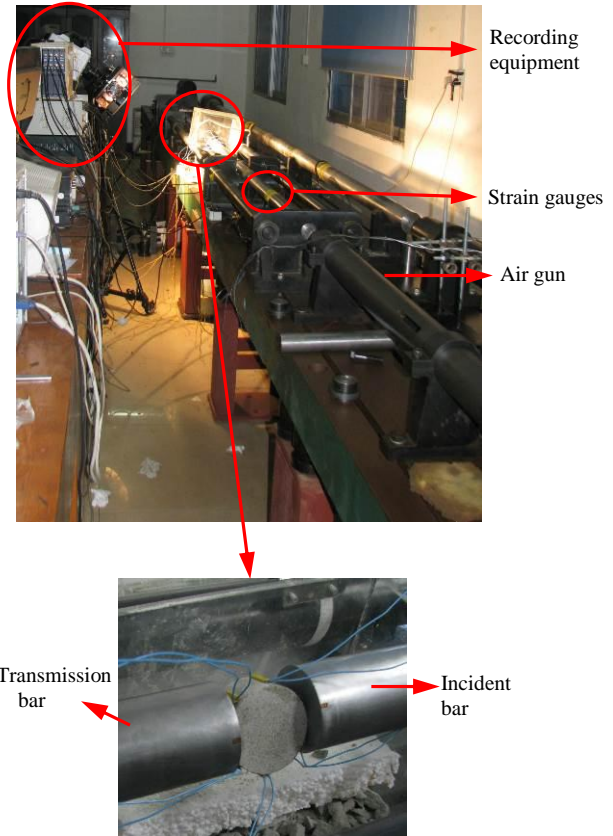


FIGURE 1 Experimental set-up for SHPB at CSU

During a SHPB test, two basic requirements must be satisfied: the specimen is under one-dimensional stress and the specimen is in-loaded evenly [10]. The equation of motion can be written as:

$$\rho \frac{\partial^2 u}{\partial t^2} = E \frac{\partial^2 u}{\partial x^2} , \quad (3)$$

where *u* is the location of the infinitesimal at *x* under stress; *E* is the elastic modulus of bars; *ρ* is the density of the bar; *t* is the time of stress loading; *x* is the location of the infinitesimal.

The half-sine wave produced by the conical bullet lengthens the rise time of the incident stress wave, allowing the specimen to be in-loaded evenly during the rise time. Since the strains in the incident and transmission bars are known, the dynamic loading forces (*P*) at the two elastic bars/ specimen interfaces may be calculated as [11]:

$$P_1 = E_b A_b (\epsilon_1 + \epsilon_R) , P_2 = E_b A_b \epsilon_T , \quad (4)$$

where  $E_b$  is the elastic bar's Young's modulus,  $A_b$  is the cross section area of the elastic bars,  $\varepsilon_i$  and  $\varepsilon_r$  are the incident and reflected strains measured by the strain gauges on the incident bar, and  $\varepsilon_T$  is the transmitted strains measured by the strain gauges on the transmission bar.

If the dynamic forces ( $P_1$  and  $P_2$ ) on both sides of the specimen are almost equal during the entire dynamic loading period, then the specimen is said to be in stress equilibrium, and the applied force on the specimen ( $P(t)$ ) can be calculated as:

$$P(t) = \frac{1}{2}(P_1 + P_2) = \frac{1}{2}E_b A_b (\varepsilon_i + \varepsilon_r + \varepsilon_T). \quad (5)$$

The impact strain  $\varepsilon(t)$  are calculated by one-dimensional stress wave theory using the following formulas:

$$\varepsilon(t) = -\frac{2c_e}{L_S} \int_0^t \varepsilon_r(t') dt', \quad (6)$$

where  $c_e$  is the elastic wave velocity of the bars;  $L_S$  is the length of sample;  $\varepsilon_r(t)$  is the strain of the reflected stress wave at time  $t$ .

Under the condition of stress equilibrium, the dynamic tensile strength ( $\sigma_{td}$ ) can be derived by using the applied dynamic load ( $P(t)$ ) and the time-to-fracture ( $t_f$ ):

$$\sigma_{td} (\sigma_{td}) = \frac{2P(t_f)}{\pi DB}, \quad (7)$$

where  $D$  is the diameter of the BD specimens,  $B$  is the thickness of the BD specimens.

The loading rate ( $\dot{\sigma}_{td}$ ) is determined by the slope of the stress history starting from the time of stress equilibrium ( $t_{equil}$ ) and ending at the time-to-fracture ( $t_f$ ).

#### 4 Sample preparation

The rock material used in this study was fine-grained sandstone found in the Zigong region of Sichuan, China. BD tests were performed to measure surface deformation. BD testing specimens are 50 (diameter)  $\times$  20 (thickness) mm. The non-parallelism and the non-perpendicularity of specimens were both less than 0.02 mm. The specimens were grey and smooth on surface, with no distinct interspaces. The density of specimens was 2.50t/m<sup>3</sup>.

To representatively capture the time-to-fracture of the specimen, three strain gauges were mounted on the specimen surface, perpendicular to the load direction along the specimen centre line with equal spacing, as shown in Figure 2.

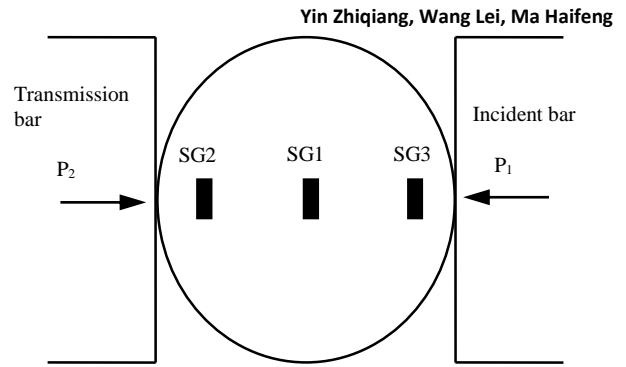


FIGURE 2 Arrangement of strain gauges on specimen

#### 5 High speed camera system

In this study, a high-speed camera (PHOTRON FASTCAM SA1.1) was used to record the full-field dynamic fracture process of specimen photographically during tests, coupled with a high-strength and non-stroboscopic light source (PALLITE VIII), positioned at a safe distance of 0.7 m from the specimen surface. The high-speed camera was operated at the setting for dynamic tests, with a frame-rate of 100,000 frame per second (10 $\mu$ s inter-frame time), and 192 $\times$ 192 pixels for size of 56 $\times$ 56 mm<sup>2</sup>. The specimen was randomly speckled with black and white paint to ensure good contrast in the digital images. The HS image of the dynamic Brazilian disk testing methods is shown in Figure 3.

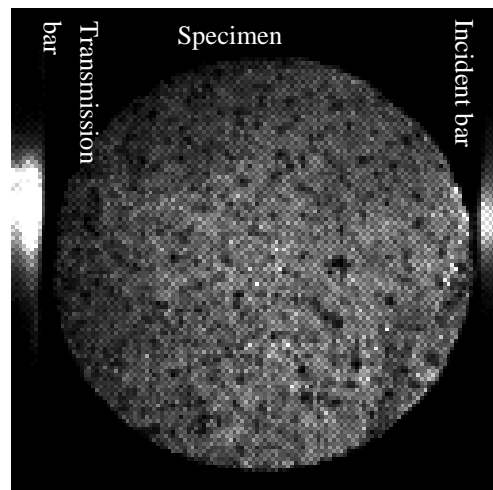


FIGURE 3 Photographic view of dynamic testing

A triggering system is composed of strain gauges on the surface of the incident bar and the oscilloscope. The incident stress wave generated by the impact of the conical bullet will propagate along the incident bar, and a TTL electrical signal will be generated when the oscilloscope detects this stress wave signal by strain gauges [12]. The camera was connected to the oscilloscope using a coaxial cable (about 2m in length). Then the camera was triggered by the TTL pulse from the oscilloscope. This pulse was generated by the strain

gauge on the incident bar, so that the number of captured images at the specimen could be obtained:

$$n = \frac{t_s - t_{in} - t_{TTL}}{t_{frame}} = \frac{t_s - s/c_e - t_{TTL}}{t_{frame}}, \quad (8)$$

where  $t_s$  is the time of the specimen HS image,  $t_{in}$  is the time of the stress wave arriving at the sample,  $s$  is the distance between the specimen and SG<sub>in</sub>,  $t_{TTL}$  is the pre trigger time by a TTL pulse, and  $t_{frame}$  is the time interval of the inter-frame.

In this test, to match the recorded images with the loading steps, the delay time from the loading start time to the triggering start time was determined to be 188 $\mu$ s. This was based on the combined consideration of the travelling time from the strain gauge to the specimen end (wave velocity 5410 m/s, distance 1017mm) and the pre-trigger time by a TTL pulse 26 $\mu$ s, as shown in Figure 4.

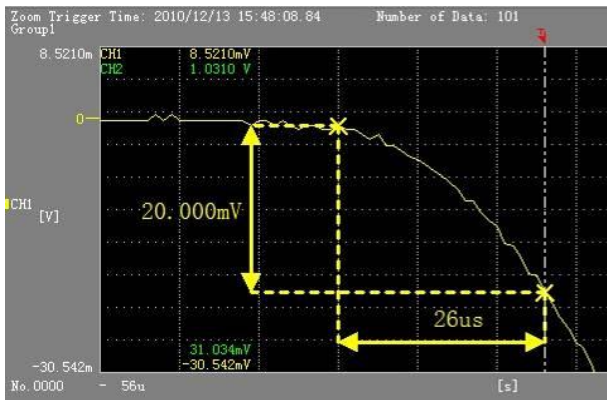


FIGURE 4 The pre trigger time measurement

## 6 Results and discussion

Figure 5 represents a typical testing result with a striking velocity of 3 m/s. Figure 6 indicates that the time of stress equilibrium was approximately 48 $\mu$ s, and the time-to-fracture was about 80 $\mu$ s, according to the time-to-peak of load and time-to-fracture of SG1. The electric potential of SG1 increased gradually from the time of stress equilibrium to the stress peak. The electric potential of SG2 and SG3 showed a similar trend, but lagged behind SG1. Therefore, it can be inferred that the cracks began at the center position (position of SG1) of the sample under dynamic loads, and extended to the two ends of the sample.

Figure 7 shows the tensile stress time history marked with corresponding points of high speed images. The dynamic tensile strength was about 14.2MPa at the loading rate of 202GPa/s.

The first image (0 $\mu$ s) was chosen as the reference image, as shown in Figure 8a. The difference images are shown in Figure 8b. The results of image difference technique reproduced the main deformation process and validate the accurate of BD test under dynamic loads. The

white spots in Figure 8b are regarded as the deformed area on the surface of the rock specimen.

Detailed observations of the patterns before 48  $\mu$ s indicate that the deformation initiated at the right end of the rock disk under dynamic loads at about 2  $\mu$ s. Then the deformation expanded leftwards and arrived at the left end of the rock disk at around 42  $\mu$ s. This result is consistent with the dynamic, photoelastic numerical simulation on the rock specimens [13].

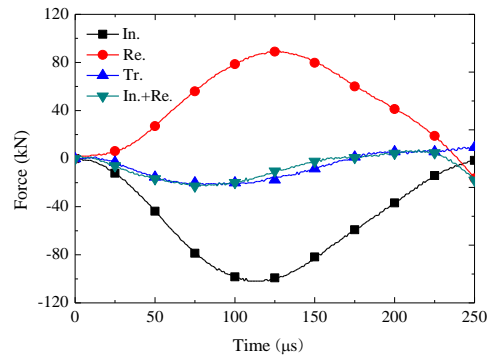


FIGURE 5 Dynamic force balance check for the dynamic Brazilian experiment

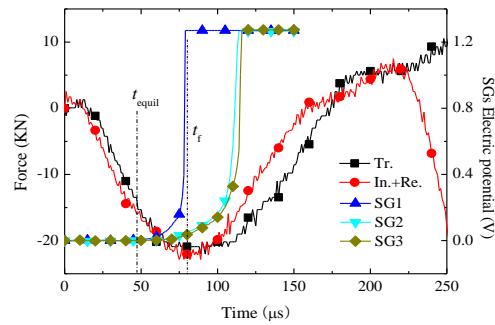


FIGURE 6 Signals from strain gauges on specimen

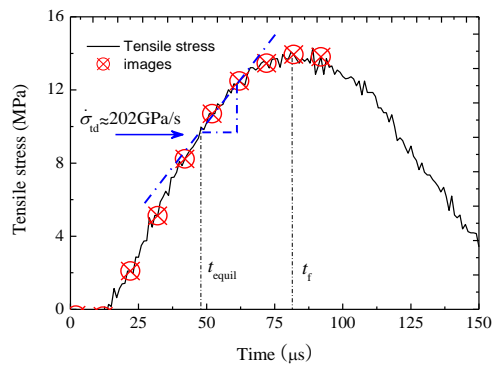


FIGURE 7 Stress-time history with high speed images

Between the time of stress equilibrium (48  $\mu$ s) and the time-to-fracture (80  $\mu$ s), white spots increased with tensile stress (Figure 7). After the time-to-fracture (80 $\mu$ s), observable cracks (block line in Figure 8b) (82  $\mu$ s, 92  $\mu$ s) were initiated at the centre of the disc along the loading line, and the tensile stress decreased with time (Figure 7). The failure pattern at time 80  $\mu$ s closely resembles the experimental results of fine-grained marble obtained by Q.B. Zhang [4].

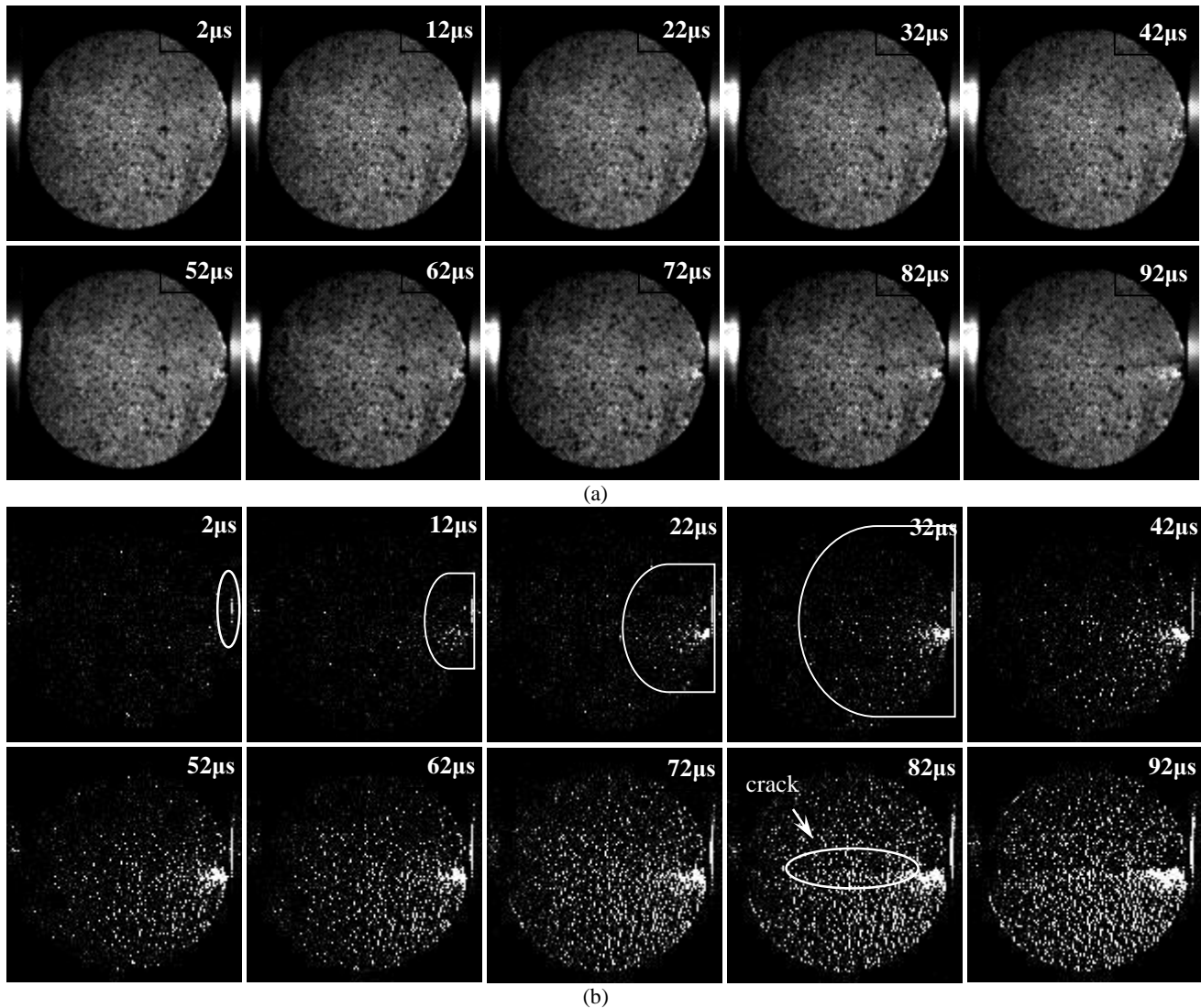


FIGURE 8 High speed images of a specimen under dynamic loading (a) Different stages; (b) Differential images

**7 Conclusions**

This study successfully employed a method combining a SHPB with an HS camera technique to explore the dynamic fracture behaviour of sandstone. In situ images of the surface of sandstone in Brazilian disk test were acquired during the dynamic loading step. The GLDD technology base on probability integration was used in conjunction with HS- photography to measure full-field deformation of specimens. The proposed system facilitates cost-effective, non-contact full-field deformation measurements of specimens in dynamic testing methods. Results demonstrate that dynamic mechanical properties can be well-determined, and that the image difference technology base on probability integration is a reliable, full-field deformation measurement method. This method is likely to gain

popularity with higher speed and higher resolution cameras as well as better computing methods, particularly as sub-pixel techniques become more readily and economically available.

**Acknowledgements**

This work was financially supported by the National Natural Science Foundation of China (NO. 51304007, 51104004, 51104068), the State Key Program of National Natural Science Foundation of China (U1361208), China Postdoctoral Science Foundation (NO. 2013M531495) and Scientific Research Fund for Young Teachers of Anhui University of Science and Technology (NO. 2012QNY39) and Scientific Research Fund for Doctor and Master of Anhui University of Science and Technology.

**References**

[1] Peters W H, Ranson W F 1982 Digital imaging techniques in experimental stress analysis *Optical Engineering* **21**(3) 427-31

[2] Song Y I, Ma S P, Yang X B 2011 Experimental investigation on failure of rock by digital speckle correlation methods *Chinese Journal of Rock Mechanics and Engineering* **30**(1) 170-5 (In Chinese)

- [3] Yin Z Q, Li X B, Yin T B 2012 Critical failure Characteristics of high stress rock inducer by impact disturbance under confining pressure unloading *Chinese Journal of Rock Mechanics and Engineering* **31**(7) 1355-62 (In Chinese)
- [4] Zhang Q B, Zhao J 2013 *International Journal of Rock Mechanics and Mining Sciences* **60**(6) 423-39
- [5] Siviour C R, Grantham S G, Williamson D M 2009 Novel measurements of material properties at high rates of strain using speckle metrology *The Imaging Science Journal* **57**(6) 326-32
- [6] Wu M, Wang H, Zhang Zh 2013 *Computer Modelling and New Technologies* **17**(4) 229-35
- [7] Bromiley P A, Thacker N A, Courtney P 2002 Non-parametric image subtraction using grey level scattergrams *Image and Vision Computing* **20**(9-10) 609-17
- [8] Li X B, Lok T S, Zhao J 2000 *International Journal of Rock Mechanics and Mining Science* **37**(7) 1055-60
- [9] Jin J F, Li X B, Zhong H B 2013 Study of dynamic mechanical characteristic of sandstone subjected to three-dimensional coupled static-cyclic impact loadings *Chinese Journal of Rock Mechanics and Engineering* **32**(7) 1358-72 (In Chinese)
- [10] Li X B, Gu D S, Lai H H 1993 On the reasonable loading stress waveforms determined by dynamic stress-strain curves of rock by SHPB *Explosion and Shock Waves* **13**(2) 125-30 (In Chinese)
- [11] Dai F, Xia K W, Tang L 2010 *International Journal of Rock Mechanics and Mining Science* **47** (3) 469-75
- [12] Zhou Z L, Li X B, Yan X M 2009 Loading condition for specimen deformation at constant strain rate in SHPB test of rocks *Chinese Journal of Rock Mechanics and Engineering* **28**(12) 2445-52 (In Chinese)
- [13] Zhu W C, Tang C A 2006 *International Journal of Rock Mechanics and Mining Sciences* **43**(2) 236-52

Authors	
	<p><b>Zhiqiang Yin, born in November, 1983, Huainan, Anhui, China</b></p> <p><b>Current position, grades:</b> Associate Professor of School of Mineral and Safety, Anhui University of Science and Technology, China.  <b>University studies:</b> D.E. in Mining Engineering at Central South University of Changsha in China.  <b>Scientific interest:</b> Rock Mechanics and Engineering.  <b>Publications:</b> More than 10 papers published in various journals.  <b>Experience:</b> Teaching experience of 10 years, 3 scientific research projects.</p>
	<p><b>Lei Wang, born in July, 1980, Huainan, Anhui, China</b></p> <p><b>Current position, grades:</b> Associate Professor of School of Mineral and Safety, Anhui University of Science and Technology, China.  <b>University studies:</b> D.E. in Safety technology and Engineering at Anhui University of Science and Technology of Huainan in China.  <b>Scientific interest:</b> Mine Dynamic Disaster  <b>Publications:</b> More than 20 papers published in various journals  <b>Experience:</b> Teaching experience of 10 years, 9 scientific research projects</p>
	<p><b>Haifeng Ma, born in August, 1984, Beijing, China</b></p> <p><b>Current position, grades:</b> Ph.D Candidate of Faculty of Resources and Safety Engineering, China University of Mining and Technology, China.  <b>University studies:</b> B.Sc. in Mining Engineering at Anhui University of Science and Technology of Huainan in China. M.Sc. at Anhui University of Science and Technology in China.  <b>Scientific interest:</b> Mine Dynamic Disaster.  <b>Publications:</b> More than 5 papers published in various journals  <b>Experience:</b> Teaching experience of 3 years, 2 scientific research projects</p>